Eur. Phys. J. B **51**, 413–419 (2006)
DOI: 10.1140/epjb/e2006-00231-9

THE EUROPEAN PHYSICAL JOURNAL B

Tunability of the Kondo effect in an asymmetrically tunnel coupled quantum dot

D. Quirion, J. Weis[a], and Klaus v. Klitzing

Max-Planck-Institut für Festkörperforschung, Heisenbergstr. 1, 70569 Stuttgart, Germany

Received 28 November 2005 / Received in final form 26 April 2006
Published online 13 June 2006 –

Abstract. The transport properties of a single quantum dot were measured at low temperature in a regime of strong asymmetric tunnel coupling to leads. By tuning this asymmetry, the two parameters of the Kondo effect in a quantum dot, the Kondo temperature and the zero-bias zero-temperature conductance, were independently controlled. A careful analysis of the Coulomb energies and of the tunnel couplings was performed. It allowed an estimate of the Kondo temperature independently of its value obtained via the temperature dependence of the conductance. Both are in good agreement. We finally compared our experimental data with an exact solution of the Kondo problem which provides the dependence of the differential conductance on temperature and source-drain voltage. Theoretical expectations fit quite well our experimental data in the equilibrium and out-of-equilibrium regimes.

PACS. 72.15.Qn Scattering mechanisms and Kondo effect – 73.21.La Quantum dots – 73.23.Hk Coulomb blockade; single-electron tunneling – 85.35.-p Nanoelectronic devices

1 Introduction

Since its observation in single quantum dots in 1998 [1–3], the Kondo effect has been measured in many different kinds of artificial structures: carbon nanotubes [4], double quantum dots [5], silicon MOSFET [6], quantum point contact [7], single atom [8] and single molecule attached to reservoirs [9], quantum antidot [10] and quantum ring [11]. It thus appears as a generic effect in nanostructures. The Kondo effect can be understood theoretically with the help of the Anderson hamiltonian which describes an electronic impurity with Coulomb repulsion coupled to Fermi-liquid reservoirs [12]. Due to the presence of a spin degeneracy in the occupation of the impurity site by electrons, electronic correlations lead at sufficiently low temperature to the screening of the spin of the impurity and the system retrieves a Fermi-liquid behaviour. Measurements have checked the main qualitative theoretical predictions on the Kondo effect: its peculiar temperature dependence, the presence of a zero-bias anomaly in the source-drain voltage characteristics independent of the gate voltage and the linear splitting of this peak with magnetic field. But oddly enough, qualitative comparisons between theoretical predictions and experiments are scarce.

Two main difficulties can be pointed out to explain this lack of comparison. First, most of the theoretical results are numerical, rendering their use quite delicate for experimentalists. Secondly, there is still a gap between the experiments which normally deal with many-electrons quantum dots, and the theoretical calculations mostly available for few-electrons system. Up to now, Goldhaber-Gordon et al. [13] have performed the most extensive comparison in the equilibrium regime (zero source-drain voltage) between experimental data and theory. Rosch et al. [14] managed to solve the Kondo problem in the limit of large magnetic field for any source-drain voltage and in the limit of large source-drain voltage for any magnetic field. They compared their results with the experimental data from Ralph and Buhrman in a single charge trap [15]. To our knowledge, this is the only comparison between theory and experiment in the non-equilibrium regime. In 1998, Schiller and Hershfield calculated for a special set of parameters an exact solution to the Kondo problem [16]. This result takes the form of an analytical formula, thus opening the possibility of a complete comparison between experimental data and theory in equilibrium and out-of-equilibrium regimes. But, to our knowledge, this comparison has not been performed yet.

In this article, we present measurements of the Kondo effect in a quantum dot asymmetrically tunnel coupled to its leads. This statement is obtained after careful extraction of the tunnel couplings to the leads via analysis of the lineshape of the Coulomb peaks (Sect. 3). In this regime of asymmetrical tunnel coupling, we were able to

[a] e-mail: j.weis@fkf.mpg.de

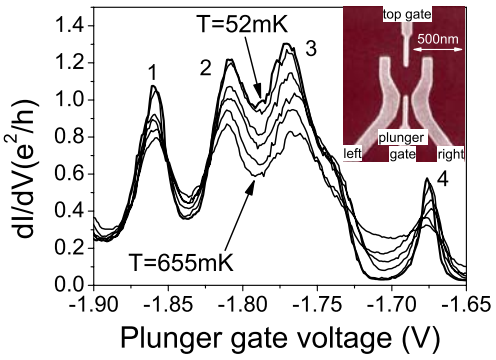

Fig. 1. Conductance versus plunger-gate voltage measured at $T = 52$ mK, 100 mK, 200 mK, 310 mK, 390 mK and 655 mK at zero source-drain voltage. The conductance in the valley between the peaks labelled with 2 and 3 decreases with increasing temperature, a behaviour characteristic of the Kondo effect. *Insert*: scanning electron microscope picture of a structure similar to the one measured.

control independently the two parameters of the Kondo effect: the zero-temperature zero-bias conductance G_0 and the Kondo temperature T_K (Sect. 4). We then deduced the Kondo temperature in two independent ways: from the temperature dependence of the zero-bias conductance, and from the couplings and Coulomb energies after the formula proposed by Haldane [17]. Comparison between the two values thus obtained lead to a very good agreement (see Sect. 5). Finally, we compared in Section 6 our experimental results in the out-of-equilibrium regime with the theoretical formula calculated by Schiller and Hershfield [16]. This formula fits our experimental curves and this questions the generality of this exact solution of the Kondo problem.

2 Description of the sample

The sample is a quantum dot based on a AlGaAs/GaAs heterostructure with the two-dimensional electron system located 50 nm underneath the surface. The mobility and electron density at 4 K are respectively 30 $m^2/(Vs)$ and $n_e = 3.2 \times 10^{15}$ m^{-2}. To define the quantum dot, a split-gate technique is used: the gate geometry is defined by electron-beam lithography and by evaporating Cr/Au electrodes. We chose a triangular geometry introduced and thoroughly studied by the group of Sachrajda et al. [18–21] (see insert Fig. 1). The effective radius of the dot is estimated to $R = 150$ nm. Thus we can geometrically estimate an upper limit for the number of electrons in the dot, $N \simeq 0.5\pi R^2 n_e = 46$, and the average level spacing $\Delta \simeq \hbar^2/m^* R^2 = 50$ μeV, with $m^* = 0.067$ m_e the electronic effective mass in GaAs. A flat disk of same radius with electrodes at infinite distance has a capacitance $C_\Sigma = 8\epsilon_0\epsilon_{\mathrm{GaAs}} R$, with $\epsilon_{\mathrm{GaAs}} = 13$ the relative dielectric constant of GaAs, leading to a Coulomb charging energy of the dot of $E_c = e^2/(2C_\Sigma) = 570$ μeV.

Each gate is dedicated to a specific role. The left and right finger gates (*left* and *right*), in reference to the top gate, are used to tune respectively the tunnel couplings to the source and to the drain. The plunger gate (*pg*) allows to control almost independently the number of electron in the dot. In the rest of this article, the top-gate voltage is fixed to –0.712 V, whereas the left and right finger-gate voltages are linearly tuned with respect to each other in the ranges [–0.690 V; –0.705 V] and [–0.490 V; –0.475 V], respectively.

The measurements were performed in a ^{3}He–^{4}He dilution fridge of present base temperature 50 mK using usual lock-in techniques with an ac-excitation $V_{ac} = 2.5$ μV rms at a frequency of 11 Hz.

3 Extraction of the tunnel couplings

In Figure 1, the conductance versus plunger-gate voltage is plotted for various temperatures[1]. Coulomb oscillations are clearly recognizable. The large conductance in the Coulomb valleys and concomitant large width of the Coulomb peaks indicate a strong tunnel coupling to the leads. In this set of parameters, the left tunnel-barrier (to source) is close to pinch-off (data not shown). Consequently, we expect a strong asymmetry between the tunnel couplings to source and drain. To check this asymmetry, we analysed the lineshape of the Coulomb peaks and their temperature dependence.

The knowledge of the tunnel couplings of a quantum dot to its leads is very important to achieve a complete control of the transport properties of the quantum dot system. Unfortunately, their determination is not always straightforward. For example, in a weak tunnel coupling regime ($\Gamma < k_B T < \Delta$), the usual two-terminal experiment does not suffice and a three-terminal geometry is needed [22].

However, when the temperature is the smallest energy scale, the expected lineshape is a thermally-broadened Lorentzian of width $\Gamma = \Gamma_S + \Gamma_D$ and of height $G_0 = (8e^2/h)\Gamma_S\Gamma_D/(\Gamma_S + \Gamma_D)^2$ at zero-temperature [23],

$$G(V_G) = G_0 \int_{-\infty}^{+\infty} L(\varepsilon, V_G)\Big[-\partial f(\varepsilon/k_B T)\Big]\, d\varepsilon \qquad (1)$$

with

$$L(\varepsilon, V_G) = \frac{(\Gamma/2)^2}{[\varepsilon - e\alpha(V_G - V_G^{res})]^2 + (\Gamma/2)^2}\,, \qquad (2)$$

$$-\partial f(\varepsilon/k_B T) = \frac{1}{4k_B T}\cosh^{-2}\left(\frac{\varepsilon}{2k_B T}\right)\,, \qquad (3)$$

where T is the electronic temperature, ∂f the derivative of the Fermi function, V_G the gate voltage used to control the number of electrons in the dot (here, the plunger

[1] The given temperature values are measured by a resistance thermometer close to the sample. The electron temperature at base temperature of the dilution refrigerator with this setup is well below 100 mK (about 50 mK) as has been checked on Coulomb blockade oscillations in the weak tunnel coupling regime.

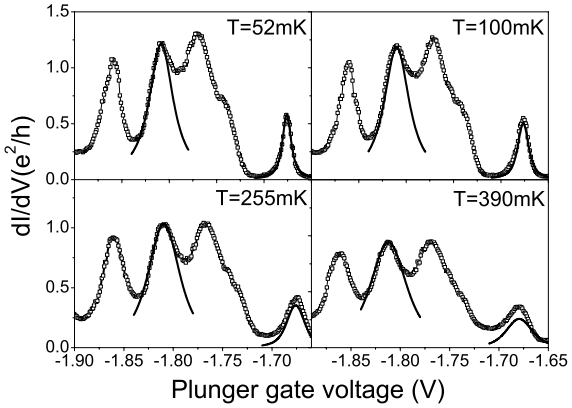

Fig. 2. Conductance versus plunger-gate voltage measured at $T = 52$ mK, 100 mK, 255 mK and 390 mK at zero source-drain voltage and corresponding fits of the peaks 2 and 4 with a thermally-broadened Lorentzian (see Eq. (1)). Parameters are given in the text.

gate voltage), V_G^{res} the gate voltage value at the resonance and α the lever-arm parameter giving the conversion between the gate voltage and the energy scales (in the following $\alpha = 5 \times 10^{-3}$; to deduce this parameter, we used the Coulomb energies: see next section). The sum and the product of the tunnel couplings are independently given by the width and the height of the Coulomb peaks. Then, resolution of a second order equation allowed us to extract the tunnel couplings Γ_S and Γ_D. To distinguish them, we used the fact that the tunnel barrier to source is closer to pinch-off than the tunnel barrier to drain.

Actually, this analysis is easily performed for the well-isolated Coulomb peak around $V_{pg} = -1.68$ V (peak 4), but may be quite more complicated for other peaks. Let us for example consider the Coulomb peak at $V_{pg} = -1.81$ V (peak 2). The conductance of the valley on its right side is not only enhanced due to the overlap of its adjacent Coulomb peaks, but also because of the Kondo effect (see next section). To obtain the right estimation of the tunnel couplings, we fitted its lineshape with a Lorentzian only on its left side. In Figure 2 are plotted the temperature dependencies of these two peaks. The agreement is good, except at the higher temperatures where the experimental data show a higher conductance than the theoretical expectation. We believe this is due to the onset at finite temperature of transport processes not included in the simple model considered above, such as transport through excited states which should occur at temperatures comparable to the mean-level spacing, $\Delta/k_B \simeq 50$ μeV$/k_B \simeq 580$ mK (see the strong increase of the conductance of the valley adjacent to peak 4).

In this gate voltage configuration, the deduced tunnel couplings to source and drain $\Gamma_S^{(i)}$ and $\Gamma_D^{(i)}$ of the peak (i) in Figure 1 are: $\Gamma_S^{(1)} = 17$ μeV and $\Gamma_D^{(1)} = 100$ μeV, $\Gamma_S^{(2)} = 30$ μeV and $\Gamma_D^{(2)} = 126$ μeV, $\Gamma_S^{(3)} = 35$ μeV and $\Gamma_D^{(3)} = 175$ μeV, $\Gamma_S^{(4)} = 4$ μeV and $\Gamma_D^{(4)} = 46$ μeV. We estimate an accuracy of around $\pm 20\%$ on these results. The tunnel couplings for each peak are different because different states are at stake. These values confirm the strong asymmetry of the tunnel coupling of the dot to its leads.

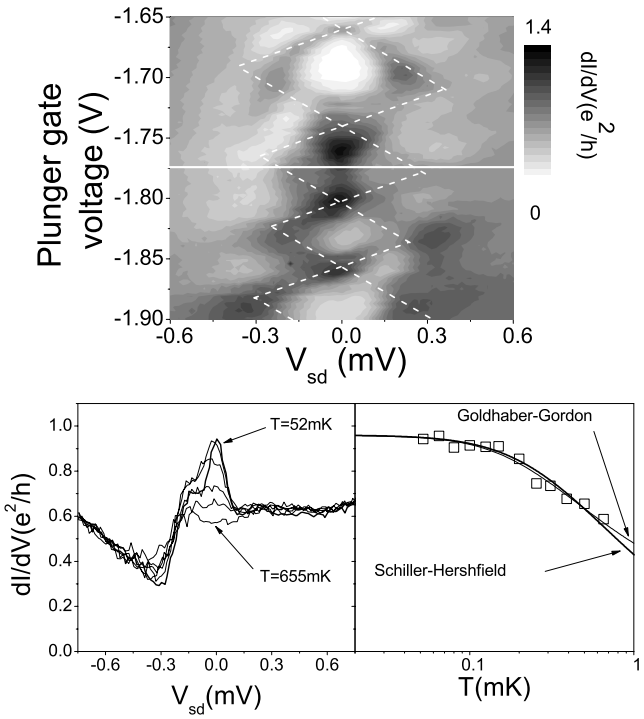

Fig. 3. *Top panel*: differential conductance versus source-drain voltage and plunger gate voltage at $T = 52$ mK. The trace (white line) crosses the middle of the valley between peak 2 and 3 of Figure 1, exhibiting a Kondo zero-bias anomaly. *Bottom panel*: (*left*) differential conductance versus source-drain voltage (white line in the top panel) measured at $T = 52$ mK, 100 mK, 200 mK, 310 mK, 390 mK and 655 mK. (*Right*) Temperature dependence of the zero-bias conductance and fits after the Goldhaber-Gordon semi-empirical formula and the Schiller-Hershfield theory (see parameters in text).

4 Tuning the Kondo effect

On the upper panel of Figure 3 the differential conductance is plotted versus source-drain voltage and plunger gate voltage, corresponding to the zero-bias measurement of Figure 1[2]. Coulomb diamonds are marked by dashed white lines. We extract the following Coulomb energies, for the valleys from top to bottom: $E_c = 180$ μeV, 140 μeV and 120 μeV. The Coulomb diamonds are smoothed as the tunnel couplings and Coulomb energies are of the same order of magnitude. But the estimate[3] deduced from Fig-

[2] The data presented in Figures 1 and 3 are measured separately. The shift of about 12 mV in the gate voltage axis between Figures 1 and 3 is presumably due to a single-electron recharging event in the vicinity of the quantum dot.

[3] The dashed lines in Figure 3 follow the peak maximum where visible. Assuming the same slope of borderlines between Coulomb blockade and single-electron-tunneling for the different electron number on the quantum dot, the probable Coulomb blockade regions are enclosed.

ure 3 is quite different from the geometrical estimate we made before (approximately 140 μeV versus 570 μeV). One can understand this discrepancy within a capacitance model. We compared the Coulomb diamond pattern of Figure 3 with one measured in a well-defined Coulomb blockade regime (data not shown). In the latter case the Coulomb energy was approximately 650 μeV, in relative agreement with the geometrical estimate. A comparison between the Coulomb diamonds allowed us to estimate that the capacitance between the dot and the source lead increased by a factor 10 between the two regimes. We believe this enhancement can explain the strong decrease of the Coulomb energy. Such a correlation between increase of tunnel couplings and decrease in Coulomb energy has already been observed by Foxman et al. [24] and was also explained in terms of increase in the capacitive coupling between the quantum dot and its leads. Such an effect was also observed by Schmid et al. while varying the tunnel coupling at constant number of electron in the dot [25].

The temperature dependence of Figure 1 shows a striking feature. Whereas the conductance of all the other Coulomb valleys increases with increasing temperature, the conductance of the valley at $V_{pg} = -1.79$ V decreases with increasing temperature. The valley marked by a white line exhibits a peak at zero-bias corresponding to this peculiar temperature dependence. It disappears as the temperature is increased (see lower panel of Fig. 3). This zero-bias anomaly is due to the Kondo effect (see next section).

Afterwards, we changed the symmetry of the tunnel couplings. To that purpose, we increased the right finger-gate voltage and to keep the number of electrons in the dot constant (maintaining the Kondo effect in this Coulomb valley), we simultaneously decrease the left finger-gate voltage linearly. Consequently, we expect a decrease of the tunnel coupling to source and an increase of the coupling to drain. The obtained differential conductance versus source-drain voltage characteristics are plotted in Figure 4. We note that the Kondo peak height decreases whereas its width seems to stay constant. This suggests qualitatively that the Kondo temperature is constant in this gate range (see next section).

5 Analysis of the Kondo effect: equilibrium regime

The Kondo effect has been under thorough studies since the first breakthrough of Jun Kondo in 1964 [26]. Its resolution appeared to be a theoretical challenge. It lead to the development of new techniques among them the renormalisation group theory [27]. As the first example of "asymptotic-free" theory, it is of prime importance in theoretical physics [28]. Due to the high technicality of the methods used to solve the Kondo problem, experiments may come as a useful support to check the validity of these methods. The observation of the Kondo effect in artificial nanostructures in 1998 [1–3] opened some new possibilities of comparison due to the high tunability of

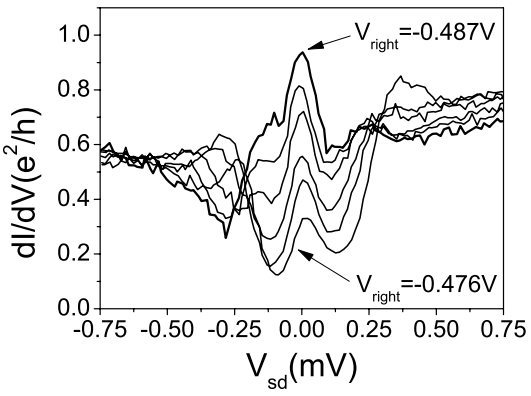

Fig. 4. Differential conductance versus source-drain voltage at $T = 52$ mK for various tunnel coupling asymmetries. From the upper to the lower curve, the tunnel coupling to drain is expected to increase and the tunnel coupling to source, to decrease.

the quantum dots. It also allowed to explore the out-of-equilibrium physics of the Kondo effect.

Direct and quantitative comparison between available data and theory is mainly hindered by the numerical nature of the theoretical predictions. Goldhaber-Gordon et al. [13] lift this problem by proposing from a theoretical curve given by Costi et al. [29] a semi-empirical fit of the form

$$G(T) = G_0 \left(\frac{T_K'^2}{T^2 + T_K'^2} \right)^s \tag{4}$$

with T the electronic temperature, $T_K' = T_K/\sqrt{2^{1/s} - 1}$ and $s = 0.22$ expected for a spin 1/2 impurity, and the zero temperature conductance $G_0 = (8e^2/h)\Gamma_S\Gamma_D/(\Gamma_S+\Gamma_D)^2$. The Kondo temperature T_K is defined by $G(T_K) = G_0/2$ and its dependence described by the Haldane formula [17]

$$k_B T_K \propto \sqrt{2\Gamma E_C}\, \exp\left[\frac{\pi\varepsilon_0(\varepsilon_0 + 2E_C)}{4\Gamma E_C} \right] \tag{5}$$

with E_C the Coulomb charging energy, ε_0 the level position in the dot ($-E_C < \varepsilon_0 < 0$) and $\Gamma = \Gamma_S + \Gamma_D$ the total tunnel coupling to the reservoirs, sum of the tunnel couplings to the source and the drain. This procedure is used in most of the experimental papers, but it does not allow analysis of out-of-equilibium data.

Schiller and Hershfield [16] managed to calculate an exact solution to the Kondo problem at a particular point in the parameter space of the Kondo hamiltonian. It assumes left and right longitudinal exchange couplings *(i)* equal and *(ii)* set to a certain value, and *(iii)* zero longitudinal exchange coupling between the two reservoirs. The exchange couplings J can be linked to the tunnel couplings with the help of the Schrieffer-Wolff transformation [30] by $1/(\rho J) = -\pi\varepsilon_0(\varepsilon_0 + 2E_C)/(4\Gamma E_C)$ with ρ the density of states of the reservoirs at the Fermi level. It should be noted that the Schrieffer-Wolff transformation, from the Anderson impurity model [12] to the Kondo model [26], generates equal longitudinal and transversal exchange couplings, which is not the case in

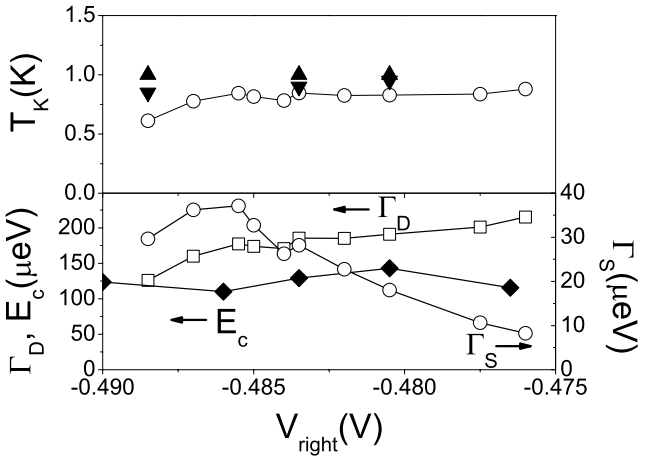

Fig. 5. *Top panel*: Kondo temperature versus right-finger gate voltage extracted from the temperature dependence of the zero-bias conductance after the Goldhaber-Gordon (upwards triangles) and Schiller-Hershfield (downwards triangles) formulae. The open squares give the Kondo temperature deduced from the parameters given on the bottom panel of this figure after the Haldane formula [17]. *Bottom panel*: Coulomb energy and tunnel couplings to leads versus right-finger gate voltage.

the Schiller-Hershfield model. Therefore, a direct comparison between the tunnel couplings extracted in this paper and the exchange couplings used by Schiller and Hershfield is difficult. At zero magnetic field, they found that the differential conductance through the quantum dot is given by

$$\partial_{V_{sd}} I(V_{sd},T) = G_0 \frac{T_K}{2\pi T} \Im m\left[\Psi^{(1)}\left(\frac{1}{2}+\frac{k_B T_K + ieV_{sd}}{2\pi k_B T}\right)\right] \quad (6)$$

with G_0 the zero-temperature zero-voltage conductance, T_K the Kondo temperature, T the electronic temperature, V_{sd} the source-drain voltage, $\Im m[\Psi^{(1)}]$ the imaginary part of the trigamma function. This formula contains only two independent parameters (G_0 and T_K), which can be extracted from the temperature dependence of the zero-bias conductance. It then allows to fit *without any free parameters* the Kondo peak in the differential conductance versus source-drain voltage characteristics. Relation (6) is a compact rewriting of another formula: the integral of a Lorentzian times the difference of the Fermi functions of the reservoirs biased by $e\,V_{sd}$. This Lorentzian is exactly the expected local density of states of a Kondo impurity at equilibrium ($V_{sd} = 0$) and zero temperature.

The temperature dependence of the zero-bias conductance is shown in the lower panel of Figure 3 and was fitted using the formulae of Goldhaber-Gordon and Schiller-Hershfield (Eqs. (4) and (6)). The deduced parameters are respectively for the two fits $T_K = 1$ K, $G_0 = 0.96$ e^2/h and $T_K = 0.85$ K, $G_0 = 0.96$ e^2/h. The two approaches give close results. The differences can be explained by the different shapes of the two theoretical predictions in the temperature regime below the Kondo temperature.

To understand the behaviour shown in Figure 4, we extracted the Coulomb energies, the tunnel couplings to the leads and the Kondo temperature corresponding to peak 2 in the same manner as explained before (results shown in Fig. 5). Within the errors bars, the Coulomb energy stays constant around 125 μeV to 150 μeV in this gate voltage range. The tunnel coupling to drain increases monotonously from 130 μeV to 215 μeV, whereas the tunnel coupling to source decreases by a factor 4, from 40 μeV down to 10 μeV (see lower panel of Fig. 5). This is the behaviour we expected from the gate voltage tuning performed here.

We have now all the parameters at hand to calculate the Kondo temperature from the Haldane formula (see Eq. (5)). To check its relevance in our experimental configuration, we measured the temperature dependency in three different asymmetry configurations, at $V_{right} = -0.4885$ V, -0.4835 V and -0.4805 V. Each time, we deduced the Kondo temperature from the temperature dependence of the zero-bias conductance fitted by the formulae of Goldhaber-Gordon and Schiller-Hershfield (Eqs. (4) and (6)). The six obtained Kondo temperatures are plotted on the upper panel of Figure 5 (upwards triangles after Goldhaber-Gordon formula and downwards triangles after Schiller-Hershfield formula). They are almost all equal around 0.9 K to 1 K, confirming the first visual impression of Figure 4. We then linearly interpolated for the intermediate (not measured) values the Coulomb energies and calculated with the Haldane formula (Eq. (5)) the expected Kondo temperature from the tunnel couplings evaluated above. We obtained a very good agreement with the three experimental values by using for the proportionality factor $\frac{1}{2}$ (see also [13]): $k_B T_K = \frac{1}{2}\sqrt{2\Gamma E_C}\,\exp(-\pi E_C/4\Gamma)$ in the middle of the Kondo valley (see upper panel of Fig. 5). We want to stress this agreement in spite of the possible multi-level configuration of the quantum dot. The satellite peak observed around $V_{sd} = 130$ μV might be a hallmark of a multi-level Kondo effect [31].

Can we now understand the behaviour observed in Figure 4? In a regime of strong asymmetric tunnel coupling ($\Gamma_S \ll \Gamma_D$), the Kondo temperature in the middle of the Kondo valley can be approximated by $k_B T_K \simeq \frac{1}{2}\sqrt{2\Gamma_D E_C}\,\exp(-\pi E_C/4\Gamma_D)$. The Kondo temperature depends only on the Coulomb energy and the stronger coupled tunnel barrier. In the experimental situation studied here, these two energies are close to each other (actually, the sample is almost in the mixed-valence regime): the exponential term of the Kondo temperature is less sensitive to small variations of them. Moreover E_C and Γ_D are almost constant in the studied gate voltage range, then the Kondo temperature is also constant. This behaviour can be seen on top panel of Figure 5. Within the same strong asymmetric regime, the zero-temperature conductance can be written: $G_0 \simeq (2e^2/h)\,\Gamma_S/\Gamma_D$. The tunnel coupling to source exhibits the most drastic change (divided by a factor 4, see lower panel of Fig. 5) and consequently drives the change of the Kondo peak height. In this regime, the Kondo temperature and the zero-bias zero-temperature conductance can be considered as independently controlled by the tunnel couplings to drain and to source, respectively.

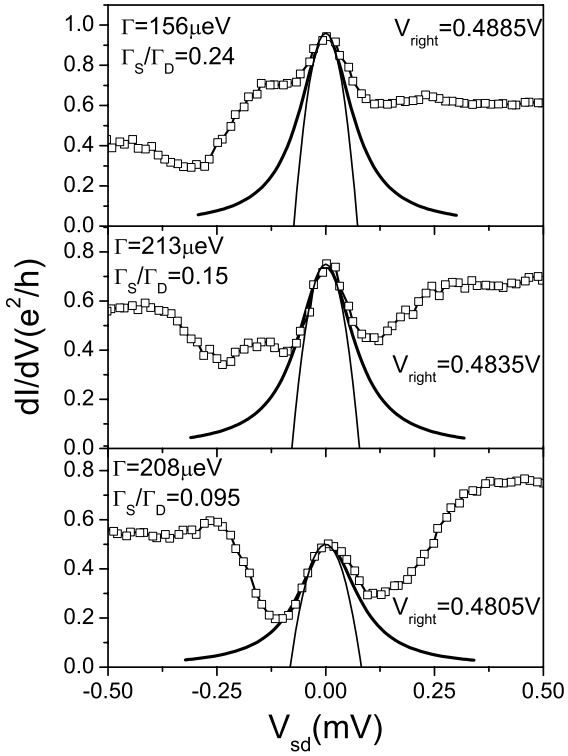

Fig. 6. *Top panel*: differential conductance versus source-drain voltage around $T = 55$ mK measured in the middle of the Kondo valley for three different tunnel coupling configurations. For the parameters of the curves from top to bottom, we extracted from the temperature dependence of the zero-bias conductance the following parameters: $T_K = 0.85$ K and $G_0 = 0.96$ e^2/h, $T_K = 0.9$ K and $G_0 = 0.75$ e^2/h, $T_K = 0.95$ K and $G_0 = 0.5$ e^2/h. The experimental curves shown on this figure are then plotted with these values with the Schiller-Hershfield formula (Eq. (6), thick lines) and a Fermi-liquid description (thin lines, see text) without any free parameter. The total tunnel coupling and the ratio of source to drain tunnel couplings extracted from the lineshapes of the Coulomb peaks are also given for information.

6 Analysis of the Kondo effect: out-of-equilibrium regime

In Figure 6, the differential conductance is plotted versus source-drain voltage in three different tunnel couplings configurations. These three configurations are those for which we performed the temperature dependence mentioned above. Consequently, the Kondo temperature T_K and the zero-temperature conductance G_0 are known and the curves in Figure 6 can be fitted without any free parameters with the Schiller-Hershfield theory (see Eq. (6) and thick lines in Fig. 6).

The agreement is quite good, except at $\Gamma_S/\Gamma_D = 0.24$, where the shoulder around $V_{sd} = -141$ μV is not understood. It is even better than the expected universal behaviour: $G(V_{sd}) = G_0[1 - (eV_{sd}/k_BT_K)^2]$ (see Fig. 5, thin lines). All Kondo-like curves should follow this scaling behaviour at low source-drain voltage and low temperature: since in this regime the spin of the impurity site is screened by the correlations with the reservoirs, a Fermi-liquid behaviour is retrieved. The agreement with the Schiller-Hershfield theory actually extends to larger source-drain voltage than the universal behaviour in our experimental situation. As the temperature is increased, the Kondo peak height diminishes as expected and the agreement lowers. At the highest measured temperature (but still lower than the Kondo temperature), the Kondo peak is not visible anymore and it seems only to fill the Coulomb gap (see for example left lower panel of Fig. 3).

Although there is an obvious agreement between the experimental data and the description by relation (6), several questions arise: the solution of Schiller and Hershfield for the Kondo problem is exactly valid for a certain set of parameters expressed in terms of exchange couplings. In a later paper, Majumdar, Schiller and Hershfield [32] analysed the deviations from this exact solution as one wanders slightly away from the solvable parameter set: relation (6) seems to hold. In our experimental situation, a large asymmetry in the tunnel couplings is present, with the consequence that we are probably rather far away from a parameter set for which relation (6) is exactly derivable. Most important, the solution obtained by Schiller and Hershfield [16] does not take into account any charge fluctuations. Consequently, it should be a valid description for quantum dots with large on-site Coulomb interaction, weakly coupled to leads. The experimental configuration studied here is the complete opposite case: the Coulomb energy is comparable to the level width Γ. Despite of this, relation (6) seems to be a good starting point for analysing experimental data.

7 Conclusion

To conclude, we studied the Kondo effect in a quantum dot asymmetrically coupled to its leads. This assertion is supported by a careful analysis of the lineshapes of the Coulomb peaks. Tuning the asymmetry of the tunnel coupling, we were able to change the height of the Kondo peak without changing the Kondo temperature. This behaviour can be explained by the strong asymmetry of the tunnel coupling. The estimate of the tunnel couplings allowed us to calculate the Kondo temperature from the usual Haldane formula and to obtain a good agreement with the experimental measurements. Finally, we compared our experimental data in the out-of-equilibrium regime without any free parameters to an exact solution of the Kondo problem and found good agreement, although its validity for our experimental situation is not proven. Further comparisons between experiment and theory are required. A guideline for such a comparison is presented here.

The authors would like to thank Avraham Schiller, Stefan Kehrein and Karsten Held for fruitful discussions, Ulrike Waizmann, Monika Riek and Frank Schartner for technical support, and Maik Hauser and Karl Eberl for providing the heterostructure. This work was supported by the BMBF project 01 BM 915/1.

References

1. D. Goldhaber-Gordon, H. Shtrikman, D. Mahalu, D. Abusch-Magder, U. Meirav, M.A. Kastner, Nature **391**, 156 (1998)
2. S.M. Cronenwett, T.H. Oosterkamp, L.P. Kouwenhoven, Science **281**, 540 (1998)
3. J. Schmid, J. Weis, K. Eberl, K. von Klitzing, Physica E **256–258**, 182 (1998)
4. J. Nygård, D.H. Cobden, P.E. Lindelof, Nature **408**, 342 (2000)
5. H. Jeong, A.M. Chang, M.R. Melloch, Science **293**, 2221 (2001)
6. M. Specht, M. Sanquer, S. Deleonibus, G. Guéguan, Eur. Phys. J. B **26**, 503 (2002)
7. S.M. Cronenwett, H.J. Lynch, D. Goldhaber-Gordon, L.P. Kouwenhoven, C.M. Marcus, K. Hirose, N.S. Wingreen, V. Umansky, Phys. Rev. Lett. **88**, 226805 (2002)
8. J. Park, A.N. Pasupathy, J.I. Goldsmith, C. Chang, Y. Yaish, J.R. Petta, M. Rinkoski, J.P. Sethna, H.D. Abruna, P.L. McEuen, D.C. Ralph, Nature **417**, 722 (2002)
9. W. Llang, M.P. Shores, M. Bockrath, J.R. Long, H. Park, Nature **417**, 725 (2002)
10. M. Kataoka, C.B.J. Ford, M.Y. Simmons, D.A. Ritchie, Phys. Rev. Lett. **89**, 226803 (2002)
11. U.F. Keyser, C. Fühner, S. Borck, R.J. Haug, M. Bichler, G. Abstreiter, W. Wegscheider, Phys. Rev. Lett. **90**, 199601 (2003)
12. P.W. Anderson, Phys. Rev. B **124**, 41 (1961)
13. D. Goldhaber-Gordon, J. Göres, M.A. Kastner, H. Shtrikman, D. Mahalu, U. Meirav, Phys. Rev. Lett. **81**, 5225 (1998)
14. A. Rosch, J. Paaske, J. Kroha, P. Wölfe, Phys. Rev. Lett. **90**, 076804 (2003)
15. D.C. Ralph, R.A. Buhrman, Phys. Rev. Lett. **72**, 3401 (1994)
16. A. Schiller, S. Hershfield, Phys. Rev. B **58**, 14978 (1998); Phys. Rev. B **51**, 12896 (1995)
17. F.D.M. Haldane, Phys. Rev. Lett. **40**, 416 (1978); note 10
18. M. Ciorga, A.S. Sachrajda, P. Hawrylak, C. Gould, P. Zawadzki, S. Jullian, Y. Feng, Z. Wasilewski, Phys. Rev. B **61**, R16315 (2000)
19. M. Ciorga, A. Wensauer, M. Pioro-Ladriere, M. Korkusinski, J. Kyriakidis, A.S. Sachrajda, P. Hawrylak, Phys. Rev. Lett. **88**, 256804 (2002)
20. J. Kyriakidis, M. Pioro-Ladriere, M. Ciorga, A.S. Sachrajda, P. Hawrylak, Phys. Rev. B **66**, 035320 (2002)
21. M. Evaldsson, I.V. Zozoulenko, M. Ciorga, P. Zawadzki, A.S. Sachrajda, e-print `arXiv:cond-mat/0306327` (2003)
22. R. Leturcq, D. Graf, T. Ihn, K. Ensslin, D.D. Driscoll, A.C. Gossard, Europhys. Lett. **67**, 439 (2004)
23. C.W.J. Beenakker, Phys. Rev. B **44**, 1646 (1991)
24. E.B. Foxman, P.L. McEuen, U. Meirav, N.S. Wingreen, Y. Meir, P.A. Belk, N.R. Belk, M.A. Kastner, Phys. Rev. B **47**, 10020 (1993)
25. J. Schmid, J. Weis, K. Eberl, Physica E **6**, 375 (2000)
26. J. Kondo, Prog. Theoret. Phys. **32**, 37 (1964)
27. K.G. Wilson, Rev. Mod. Phys. **47**, 773 (1975)
28. P. Coleman, Ann. Henri Poincaré **4**, S559 (2003); e-print `arXiv:cond-mat/0307004` (2003)
29. T.A. Costi, A.C. Hewson, V. Zlatic, J. Phys.: Condens. Matter **6**, 2519 (1994)
30. J.R. Schrieffer, P.A. Wolff, Phys. Rev. **149**, 491 (1966)
31. T. Inoshita, A. Shimizu, Y. Kuramoto, H. Sasaki, Phys. Rev. B **48**, 14725 (1993); T. Inoshita, Y. Kuramoto, H. Sasaki, Superlattices Microstruct. **22**, 75 (1997)
32. K. Majumdar, A. Schiller, S. Hershfield, Phys. Rev. B **57** 2991 (1998)